

# 14C.1 ON THE IMPORTANCE OF THE NONTRADITIONAL CORIOLIS TERMS IN LARGE-SCALE MOTIONS ASSOCIATED WITH CUMULUS CONVECTIVE FORCING IN THE TROPICS: FORCED RESPONSE PROBLEM

Michiya Hayashi\* and Hisanori Itoh  
Kyushu University, Fukuoka, Japan

## 1. INTRODUCTION

Atmospheric motions are represented by a series of equations including the momentum equation. Because the accurate form of these equations is so complex, it is often necessary to use their approximated forms. In the hydrostatic primitive equations (HPEs), which is most frequently used in numerical models, the shallow atmosphere approximation is used, in which the practical thickness of the atmosphere is acknowledged to be much thinner than the mean radius of the solid earth ( $a \approx 6370$  km). When using this approximation, however, the “traditional approximation” (TA) must be used; in the momentum equations, two cosine Coriolis terms originated from the meridional component of the earth’s rotation vector (hereafter, *nontraditional Coriolis terms* or NCTs) and some metric terms are eliminated so as not to violate any fundamental physical principles, such as the conservative law of angular momentum (Gerkema et al. 2008).

However, some studies have suggested that near the equator where the cosine factor is large, the TA may not be appropriate (e.g., White and Bromley 1995, hereafter, WB95). WB95 indicated that since diabatic heating due to cumulus convection involves air mass ascent in the tropics, the NCT associated with vertical motion in the zonal momentum equation may become too large to be neglected. However, no published study has determined the effect of the NCTs interacting with diabatic heating in the cumulus-active tropics. Thus, in this study, we quantitatively investigate the effect of the NCTs on large-scale motions. As its first step, we treat motions forced by local positive-only diabatic heating mimicking cumulus heating near the equator.

## 2. GOVERNING EQUATIONS

We use the three-dimensional quasihydrostatic equations (QHEs) formulated by WB95. The

equations used are approximated on an equatorial  $\beta$ -plane, and are linearized, i.e.,

$$\frac{\partial u}{\partial t} = \beta y v - 2\Omega w - C_p \bar{\theta} \frac{\partial \pi'}{\partial x} - \gamma u + K \nabla^2 u, \quad (1)$$

$$\frac{\partial v}{\partial t} = -\beta y u - C_p \bar{\theta} \frac{\partial \pi'}{\partial y} - \gamma v + K \nabla^2 v, \quad (2)$$

$$C_p \bar{\theta} \frac{\partial \pi'}{\partial z} - \frac{g}{\bar{\theta}} \theta' = 2\Omega u, \quad (3)$$

$$\frac{\partial \theta'}{\partial t} = -w \frac{d\bar{\theta}}{dz} - \gamma \theta' + \frac{\dot{Q}}{C_p \bar{\pi}}, \quad (4)$$

$$\frac{\partial \rho'}{\partial t} = -\bar{\rho} \left( \frac{\partial u}{\partial x} + \frac{\partial v}{\partial y} + \frac{\partial w}{\partial z} - \frac{w}{H} \right), \quad (5)$$

$$\frac{\rho'}{\bar{\rho}} + \frac{\theta'}{\bar{\theta}} + \left( 1 - \frac{1}{\kappa} \right) \frac{\pi'}{\bar{\pi}} = 0, \quad (6)$$

where symbols are conventional except that  $\dot{Q}$  is diabatic heating,  $\pi \equiv (p/p_s)^\kappa$  Exner function ( $p_s \equiv 1000$  hPa is surface pressure of the basic state),  $\Omega$  the angular speed of the earth’s rotation,  $\gamma$  the Rayleigh damping/Newtonian cooling coefficient,  $K$  the horizontal diffusion coefficient, and  $H$  a scale height. The overbars and primes indicate basic states depending on  $z$  only and perturbations, respectively. Since no basic flow is assumed, all the velocity fields are perturbed quantities. We assume that the temperature of the basic state is  $T_s$  ( $= 300$  K) at the surface, having a constant lapse rate  $\Gamma$  below the altitude of the tropopause  $z_h$  ( $= 15$  km) and being constant above  $z_h$ .

In the QHEs, the spherical geopotential approximation is assumed and the vertical acceleration term in the vertical momentum equation is eliminated. This allows  $w$  to be diagnostically determined. The NCTs are retained in the zonal momentum equation (1) and the quasihydrostatic equation (3). Note that even for the linearized QHEs without basic flow, it is impossible to separate the vertical and horizontal structure equations (Gerkema et al. 2008). Gill and Phillips (1986) demonstrated that the nonlinear effect of the response to diabatic heating is weak enough to retain the pattern obtained by using the linearized HPEs (Gill 1980).

\*Corresponding author address: Michiya Hayashi, Dept. of Earth and Planetary Sciences, Graduate School of Sciences, Kyushu Univ., 6-10-1 Hakozaki, Higashi-ku, Fukuoka 812-8581, Japan; e-mail: m-hayashi@weather.geo.kyushu-u.ac.jp

### 3. NUMERICAL CALCULATIONS

Prescribed forcing  $\dot{Q}(x, y, z, t)$  is supposed to move eastward with a constant frequency  $\omega$ . The equatorially symmetric and local positive-only diabatic heating mimicking cumulus convection is given by

$$\frac{\dot{Q}}{C_p} \equiv Q_a \cos \frac{\pi y}{H_y} \cos \frac{\pi x}{H_x} \sin \frac{\pi z}{z_h} e^{z/2H} e^{-i\omega t} \quad (7)$$

when  $|y| < H_y/2$ ,  $|x| < H_x/2$  and  $0 < z < z_h$ , otherwise  $\dot{Q}/C_p \equiv 0$ . Here  $H_x$  and  $H_y$  are the zonal and meridional lengths of the heating, respectively. The factor  $\exp(z/2H)$  denotes the effect due to the density stratification of the basic state.  $Q_a$  is assigned a value which gives  $10 \text{ K d}^{-1}$  at its maximum. Then, by replacing  $\partial/\partial t$  to  $-i\omega$  in (1)–(6), the equations become “independent” of time, as all the variables responding to the forcing have the same time dependency.

The boundary condition in the zonal direction is cyclic. The equatorial symmetry is assumed in the meridional direction since equatorially symmetric forcing is used. The boundary condition in the meridional direction is then given by  $v = 0$ ,  $\partial u/\partial y = \partial \pi/\partial y = 0$  at  $y = 0$  (equator) and  $Y$  (northern boundary). The boundary condition in the vertical direction is  $w = 0$  at  $z = 0$  and  $\pi = 0$  at  $z = z_t$  (model top). The model domain is  $2\pi a$  in the zonal direction,  $4000 \text{ km}$  ( $= Y$ ) northward from the equator in the meridional direction, and  $45.5 \text{ km}$  ( $= z_t$ ) from the surface in the vertical direction. The respective grid intervals of the zonal, meridional, and vertical directions are  $\Delta x \approx 156 \text{ km}$  (256 grids corresponding to the maximum zonal wavenumber  $K_m = 128$  for a spectral expansion in the zonal direction),  $\Delta y = 125 \text{ km}$  and  $\Delta z = 1 \text{ km}$ . The time constant of  $\gamma$  is set at 2 days from the surface to 1 km height, and 10 days between 1 and 30 km; above 30 km, height-dependent values vary linearly, reaching a value of 1 day at  $z_t$ . The time constant of  $K$  is 18 hours at the maximum wavenumber.

As shown below, the meridionally localized forcing is crucial in determining the effects of the NCTs. Therefore, results of two numerical calculations with different horizontal scales of the equatorially symmetric heating (i.e.,  $H_x$  and  $H_y$ ) are shown and compared here: (i) both  $H_x$  and  $H_y$  are 2000 km (hereafter, Square experiment; SQ), and (ii)  $H_x$  is 2000 km but  $H_y$  is 1000 km (hereafter, REctangular experiment; RE). We consider eastward moving forcing with a 50-day period, that is,  $\omega = 2\pi/(50 \text{ d})$ , as an intraseasonal frequency. Results with and without the NCTs have

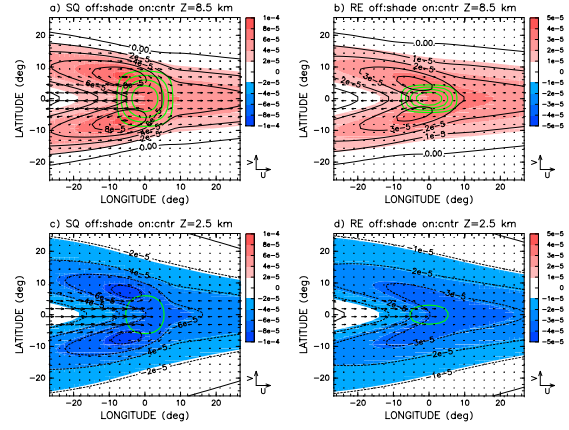


Figure 1. Exner function perturbation off-value (shade) and on-value (contour), horizontal wind off-value (vector), and diabatic heating (green contour) at 8.5 km height (top) and 2.5 km height (bottom) in each experiment. (a) and (c) represent SQ, and (b) and (d) represent RE. The wind scale is indicated in the bottom right corner of each panel, which represents  $5 \text{ m s}^{-1}$ . The vertical and horizontal axes denote latitude and longitude, respectively. The Exner function perturbation is shaded and contoured every  $2 \times 10^{-5}$  for (a) and (c), and  $1 \times 10^{-5}$  for (b) and (d). The contour interval of diabatic heating is  $2 \text{ K d}^{-1}$ .

been determined and comparisons made.

Hereafter, perturbations obtained from the equations with and without the NCTs are referred to as *on-value* and *off-value*, respectively. The term *contribution* is defined as the subtraction of the off-value from the on-value, which then signifies the effect of the NCTs. As indicated by (1)–(6), the off-value is the solution of the HPEs. The term contribution can therefore be considered to refer to the effects which are omitted by the TA in the HPEs.

### 4. RESULTS

Figure 1 shows the horizontal patterns in SQ and RE at 8.5 km and 2.5 km height. Off- and on-values of Exner function perturbations, off-values of horizontal wind, and the forcing are presented. From the equatorial symmetry, patterns in the Southern Hemisphere are also shown for the convenience of the reader. Results relating to the off-values confirm the east-west asymmetric solution derived by Gill (1980), where a Rossby (Kelvin) response occurs at the west (east) side of the forcing. Similar structures are obtained for on-values with the NCTs (see the contours in Fig. 1).

Table 1 gives the ratio of the (absolute) maximum of the contribution to the (absolute) maximum of the off-value for each variable in SQ and RE. Because this ratio is calculated from the contribution and off-value maxima, and the point of

Table 1. Ratios of the absolute maximum of contributions to the absolute maximum of off-values of each variable ( $\pi$ ,  $u$ ,  $v$ ,  $w$ , vertical vorticity  $\zeta$ , horizontal divergence  $D$ ,  $\theta$ ,  $\rho$ ) in SQ and RE. The units are percentages (%). The sign of inequality,  $<$ , indicates that the ratio is smaller than the value presented.

	$\pi$	$u$	$v$	$w$	$\zeta$	$D$	$\theta$	$\rho$
SQ	6.6	3.3	8.8	$<0.1$	5.1	0.6	3.5	3.6
RE	11.8	10.8	19.7	$<0.1$	17.3	1.4	4.1	4.0

the maximum contribution does not generally coincide with that of the maximum off-value, the ratio of the contribution to the off-value at the point of the maximum contribution must be larger than the ratio in Table 1.

This table demonstrates that the contributions to vertical velocity  $w$  and horizontal divergence  $D$  are small in both experiments. It also confirms that contributions of these two variables are small at any point (not shown). However, the NCTs largely affect zonal velocity  $u$ , meridional velocity  $v$ , vertical vorticity  $\zeta$ , and perturbations of pressure  $\pi$ , potential temperature  $\theta$ , and density  $\rho$ . Additionally, this table also indicates that the ratios of the contributions to  $\pi$ ,  $\zeta$ ,  $u$ , and  $v$  are much larger in RE than in SQ. Although the values for  $\theta$  and  $\rho$  in both experiments and for  $u$  in SQ appear to be small, contributions to them cannot be neglected because larger contributions than these are identified at each point.

The characteristics of the contribution to  $\pi$  and  $\zeta$  are shown in Figs. 2 and 3, respectively. Note that these figures indicate the results in SQ, but similar structures are obtained in RE. The contribution to  $\pi$  ( $\zeta$ ) is positive (negative) at the west side and negative (positive) at the east side of the heating. Opposite from the off-values, the contributions have an equivalent barotropic structure standing vertically, and the altitude of the maximum contributions coincides with that of the forcing (Figs. 2a and 3a). As a result, the NCTs weaken the cyclonic pressure, and also vorticity, at lower levels and strengthen the anticyclonic pressure, and vorticity, at upper levels on the west side of the forcing (Figs. 2a and 3a).

It is also interesting that the absolute values of the contributions are much larger at the west side of the heating than at the east side. In Figs. 2b and 3b, from the comparison between the off-values (contour) and contributions (shade), the peak of the contributions located at the west side of the heating nearly coincides with that of the off-values.

On the contrary, the contributions to  $\theta$  and  $\rho$  do not represent the equivalent barotropic structure (Fig. 4), and do not exhibit the difference between two experiments (Table 1).

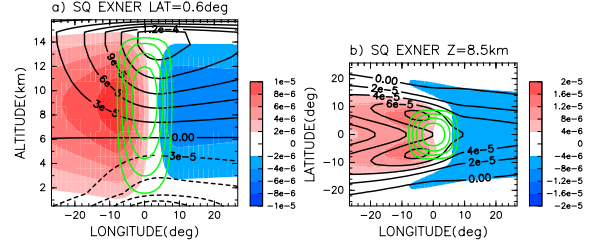


Figure 2. (a) Longitude-height cross section at 0.6°N and (b) horizontal section at 8.5 km height for the contribution to the Exner function perturbation (shade) and its off-value (contour; solid line: positive, dashed line: negative) in SQ. The green line denotes the diabatic heating (contour interval:  $2 \text{ K d}^{-1}$ ).

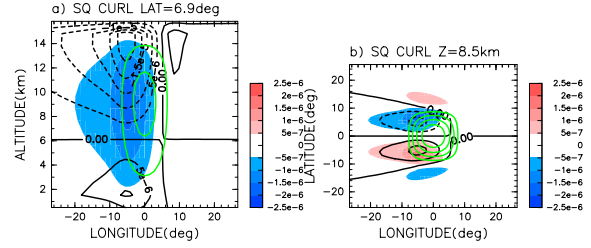


Figure 3. Same as Fig. 2 except for the vertical vorticity. Here, (a) is a cross section at 6.9°N.

## 5. DISCUSSION AND CONCLUSIONS

By giving a frequency  $\omega$  to all the variables, the linearized equations (1)–(6) are rewritten as equations for contributions by subtracting off-values from on-values. Subscripts  $c$  and  $on$  denote contribution and on-value, respectively. Horizontal diffusion terms in these equations are so small that they can be neglected without any annotation in the following consideration. The momentum equations for contributions then become

$$-i\omega u_c = \beta y v_c - 2\Omega w_{on} - C_p \bar{\theta} \frac{\partial \pi_c}{\partial x} - \gamma u_c, \quad (8)$$

$$-i\omega v_c = -\beta y u_c - C_p \bar{\theta} \frac{\partial \pi_c}{\partial y} - \gamma v_c, \quad (9)$$

$$C_p \bar{\theta} \frac{\partial \pi_c}{\partial z} - \frac{g}{\bar{\theta}} \theta_c = 2\Omega u_{on}. \quad (10)$$

On-values,  $w_{on}$  and  $u_{on}$ , appear in (8) and (10), respectively.

From  $\partial(9)/\partial x - \partial(8)/\partial y$ , the equation for the contribution to vertical vorticity  $\zeta_c$  can be obtained as

$$(-i\omega + \gamma) \zeta_c = -\beta v_c - \beta y D_c + 2\Omega \frac{\partial w_{on}}{\partial y}. \quad (11)$$

Because the contribution to horizontal divergence is small enough to be neglected, we can define the contribution to streamfunction  $\psi_c$  to be  $u_c = -\partial\psi_c/\partial y$  and  $v_c = \partial\psi_c/\partial x$  with a good approximation. The equation can then be rewritten

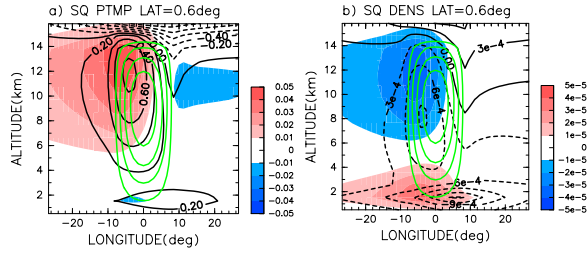


Figure 4. Same as Figs. 2a except for (a) the potential temperature perturbation and (b) the density perturbation.

as

$$\left[ \beta \frac{\partial}{\partial x} + (\gamma - i\omega) \nabla^2 \right] \psi_c \approx 2\Omega \frac{\partial w_{on}}{\partial y}. \quad (12)$$

Equation (12) gives a physical interpretation of why the NCTs generate the contribution to vertical vorticity shown in Fig. 3. On the equatorial  $\beta$ -plane approximation, the factor  $2\Omega$  on the right-hand-side is the meridional component of the planetary vorticity (i.e., cosine Coriolis component, or the planetary vorticity vector itself over the equator). This equation implies that the planetary vorticity is vertically tilted by  $\partial w_{on}/\partial y$ , generating the vertical component of relative vorticity (see Fig. 5). In the Northern Hemisphere where  $\partial w_{on}/\partial y < 0$ , negative vorticity is produced. If there were only a  $\gamma$  term on the left-hand-side, the vorticity produced would attain a maximum at the longitude where  $w_{on}$  is at its maximum. However, this negative vorticity is shifted to the west side of the heating by the  $\beta$  term. The  $-i\omega$  term makes the contribution become large in the west because this term physically implies the phase lag of the response to forcing, and the forcing is assumed to move eastward ( $\omega > 0$ ). These three terms interact to place the negative vorticity at the west side as a Rossby response. That is, the east-west asymmetry of  $\zeta_c$ , and therefore of  $\psi_c$ , is produced.

It is easily understood that  $\zeta_c$ ,  $\psi_c$ ,  $u_c$ , and  $v_c$  have the equivalent barotropic structure. These distributions are primarily determined by the strength of the tilting,  $2\Omega(\partial w_{on}/\partial y)$ . Since the structure of  $w_{on}$  is arranged vertically, these contributions also have the same vertical structure. Their amplitude maxima occur in the middle level of the troposphere corresponding to the altitude of the  $w_{on}$  maximum.

Among the variables having a large effect on the NCTs, the contributions to  $\pi$ ,  $u$ ,  $v$ , and  $\zeta$  become larger when there is a larger meridional gradient of the heating, i.e., in RE. Equation

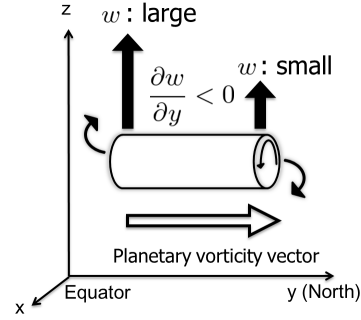


Figure 5. Schematic diagram of the tilting of the planetary vorticity. The cylinder and upward thick arrows respectively denote the vortex tube, which has the planetary vorticity, and vertical motion. In the Northern (Southern) Hemisphere, the planetary vorticity vector is tilted downward (upward) by the negative (positive) meridional gradient of the vertical velocity.

(12) demonstrates that the larger the meridional gradient of heating ( $\partial \dot{Q}/\partial y \sim \partial w_{on}/\partial y$ ) is, the larger the contributions become. As stated above,  $\partial w_{on}/\partial y$  determines the strength of tilting of the horizontal planetary vorticity so that  $\zeta_c$  becomes larger at larger gradients of heating. Furthermore, both  $u_c$  and  $v_c$  being closely related to  $\zeta_c$  ( $\psi_c$ ) also have a strong dependence on the meridional gradient of heating. Since the horizontal winds tend to adjust the pressure,  $\pi_c$  also shows the same character.

In summary, the effect of the NCTs near diabatic heating appears as the tilting of the planetary vorticity due to the meridional gradient of the vertical velocity. The vertical vorticity produced by the tilting adjusts the pressure. Thus, vertical vorticity (horizontal winds) and pressure perturbation are strongly affected by the NCTs. Contributions to them have the equivalent barotropic and east-west asymmetric structure. In addition, contributions to them become large when the meridional gradient of heating is large. As future work, we will investigate the effect of the NCTs using a time-evolution model.

## REFERENCES

- Gerkema, T., J. T. F. Zimmerman, L. R. M. Maas, and H. van Haren, 2008: Geophysical and astrophysical fluid dynamics beyond the traditional approximation. *Rev. Geophys.*, **46**, RG2004.
- Gill, A. E., 1980: Some simple solutions for heat-induced tropical circulation. *Quart. J. Roy. Meteor. Soc.*, **106**, 447-462.
- , and P. J. Philips, 1986: Nonlinear effects on heat-induced circulation of the tropical atmosphere. *Quart. J. Roy. Meteor. Soc.*, **112**, 69-91.
- White, A. A. and R. A. Bromley, 1995: Dynamically consistent, quasi-hydrostatic equations for global models with a complete representation of the Coriolis force. *Quart. J. Roy. Meteor. Soc.*, **121**, 399-418.